Microchimica Acta (2020) 187:97
https://doi.org/10.1007/s00604-019-4095-0

ORIGINAL PAPER

Target induced framework nucleic acid nanomachine with doxorubicin-spherical nucleic acid tags for electrochemical determination of human telomerase activity

Yong Shen[1] · Jiaomei Gong[2] · Qingxia Xu[1] · Lili Zhou[1] · Jiahe Sheng[1]

Received: 21 July 2019 / Accepted: 23 December 2019

Abstract

A stable and enzyme-free method is described for highly sensitive determination of telomerase activity. It is based on the use of a framework nucleic acid (FNA) nanomachine and doxorubicin-spherical nucleic acid (DSNA) tags. Upon incubation with telomerase, the primer-tetrahedron becomes elongated to form the handed swing arm. The extended swing arm autonomously moves along the predefined track consisting of entropy-tetrahedron by consecutive strand displacement under the aid of fuel-tetrahedron. As a result, many (entropy-tetrahedron)-(fuel-tetrahedron) complexes are assembled for combining the DSNA tags. This results in an amplified electrochemical signal, typically measured at around −0.63 V (Ag/AgCl). The use of an enzyme-free FNA nanomachine and of DSNA tags warrants outstandingly high stability and sensitivity. The method shows a broad dynamic correlation of telomerase activity in cell extracts. The analytical range extends from 10 to 1.0×10^4 HeLa cells mL^{-1} with a lower detection limit of 2 cells mL^{-1}. The differences in telomerase activity between different cancer cells can be easily evaluated. The method was further verified by quantifying telomerase activity of cancer cells in accumulated normal cells. Therefore, the sensing method has great potential for clinical application.

Keywords Biosensor · Tetrahedron · Entropy-driven circuit · Isothermal signal amplification · Spherical nanoparticle core · Nucleic acid shell · Square wave voltammetry · Cyclic voltammetry · Electrochemical impedance spectroscopy

Introduction

Telomerase is a ribonucleoprotein complex and can extend telomeric repeats $(TTAGGG)_n$ onto the 3′-end of telomers [1]. Telomer length gradually shortens along with the natural cell division, leading to cellular aging and senescence [2]. To date, telomerase is over-expressed in over 85% of tumor cells, and it has become a promising diagnostic and prognostic tumor biomarker [3]. Therefore, it is crucial to detect telomerase activity for early cancer diagnosis and treatment. Many biosensing methods have been developed to evaluate telomerase activity, such as fluorescence [4–7], colorimetry [8, 9], and electrochemistry [10, 11] et al. Among them, electrochemical techniques have attracted considerable attention owing to low costs and rapid response [12].

Nucleic acids have been used to build diverse accurate signal amplification strategies and nanomachines for biosensing and biomedicine, due to excellent predictability and specificity of Watson-Crick base pairing [13, 14]. For one thing, signal amplification strategies have been widely used to detect telomerase activity, such as loop-mediated isothermal amplification (LAMP) [15], rolling circle amplification (RCA) [16], and strand displacement reaction [17, 18]. For another thing, The DNA nanomachines can execute mechanical movement for signal amplification in constructing detection approaches [19]. For instance, enzymatic cleavage propelled DNA nanomachine was developed for the detection of telomerase activity [20]. However, these methods suffer from some disadvantages. Firstly, the involvement of protein enzymes needs to control strictly reaction conditions, which often lead to

Electronic supplementary material The online version of this article (https://doi.org/10.1007/s00604-019-4095-0) contains supplementary material, which is available to authorized users.

✉ Yong Shen
zlyyshenyong3058@zzu.edu.cn

[1] Department of Clinical Laboratory, Affiliated Cancer Hospital of Zhengzhou University, Zhengzhou 450014, Henan, China

[2] Department of Clinical Laboratory, the Second Affiliated Hospital of Zhengzhou University, Zhengzhou 450014, Henan, China

Published online: 06 January 2020

nonspecific response [21]. Secondly, the activation of protein enzymes and free DNA components may confront interferences in complex matrices. These drawbacks restrict their clinical applications. Therefore, constructing a sensing strategy for sensitive and stable evaluation of telomerase activity still remains urgently needed.

Framework nucleic acids (FNAs) including tetrahedron, polyhedron, and DNA origami etc., have been explored to develop biosensing strategies owing to structural order and high stability [22, 23]. In addition, these nanostructures can enhance target accessibility at the biosensing interface, which greatly improve sensitivity [24]. Isothermal amplifiers exhibit remarkably enhanced stability by inserting into framework nucleic acids [25, 26]. For example, the entropy-driven circuit imbedded DNA tetrahedron was reported for intracellular microRNA imaging [26]. Nevertheless, the sensitivity of the single DNA amplifier cannot meet the demand of trace analysis [27]. Faced with these challenges, we constructed a novel FNA nanomachine for enzyme-free and highly sensitive detection of telomerase activity with doxorubicin-spherical nucleic acids tags.

Spherical nucleic acids (SNAs) are comprised of spherical nanoparticle cores and oriented nucleic acid shells [28]. This structure endows nucleic acid shells with several unique features, such as low toxicity, resistance to enzymatic degradation, and improved binding constant with complementary sequences [29, 30]. Doxorubicin (DOX) has been known to be easily intercalated into a double helix of DNA [31], showing higher electrochemical signal than methylene blue. Therefore, SNAs are used to appropriate DOX carrier for electrochemical detection of telomerase.

In the presence of telomerase, the primer-tetrahedron (PT) is recognized and elongated by telomerase to form a handed swing arm. Subsequently, the extended swing arm binds to entropy-tetrahedron (ET) to expose the prelocked toehold domain. Then, fuel-tetrahedron (FT) rapidly binds to the exposed toehold domain, triggering strand displacement reaction to form ET-FT complex for capturing the doxorubicin-spherical nucleic acids (DSNA) and producing an amplified electrochemical signal. The extended swing arm is released and will start a new cycle reaction. Therefore, an enzyme-free and high stable strategy is successfully developed for highly sensitive telomerase detection. The method provides a promising tool for cancer early diagnosis.

Experimental section

Materials, reagents, apparatus, preparation of the probes, and native polyacrylamide gel electrophoresis (PAGE) are described in the Electronic Supporting Material (ESM).

The number of DOX and double-strand DNA (dsDNA) molecules per AuNP

AuNPs were synthesized in accordance with the reported method [32]. The preparation of DSNA tags is depicted in Fig. 1a. The synthesized steps of AuNPs and DSNA tags are described in the ESM. According to the previously reported method [33], the amount of DOX loaded in dsDNA was firstly evaluated. The doxorubicin loading efficiency was around 43.5%. Further, the number of dsDNA molecules on per AuNP was quantified based on the method that previously reported [34, 35]. The amount of dsDNA on each AuNP was estimated to be around 105. The specific steps of determination of the number of DOX and dsDNA molecules on per AuNP are described in the ESM.

Electrochemical determination of telomerase activity

Cell culture, extraction of telomerase, and modification of the bare gold electrode are described in the ESM. The cyclic voltammetry (CV) (from 0.2 V to 0.6 V) and electrochemical impedance spectroscopy (EIS) measurements were performed in 1.0 mM $[Fe(CN)_6]^{3-/4-}$ solution and the supporting electrolyte was 0.1 M KCl. For telomerase analysis, 8 μL of the telomerase extracts with different concentrations and 250 nM FT probes was added into the above modified gold electrode, and then incubated at 37 °C for 45 min. Finally, the electrode was immersed in DSNA tags solution at room temperature for 30 min, and then washed three times with 10 mM Tris-HCl. The square wave voltammetry (SWV) response was obtained in Tris-HCl (20 mM, pH 7.4) with potential range of −0.80 to −0.3 V with a scan rate of 50 $mV{\cdot}S^{-1}$, amplitude of 25 mV and frequency of 25 Hz.

Results and discussion

Mechanism of the method

The operation principle of the method is illustrated in Scheme 1. The sensing system only contains the self-assembled probe ET, PT and DSNA tags. The ET and PT probes are firstly immobilized on the surface of the bare gold electrode by Au-S bonds. Upon incubation of telomerase extracts with the sensing system, tandem telomeric repeat sequences (5′-TAGGG-3′) are added to the 3′ end of telomerase primer in probe PT, forming the handed swing arm. The extended swing arm recognizes the toehold domain in probe ET through accurate base pairing, and then displaces P strand by strand migration to expose the prelock toehold domain. Subsequently, the probe FT binds to the exposed toehold, which simultaneously release the R strand and the extended swing arm that start to next cycle by further hybridizing with

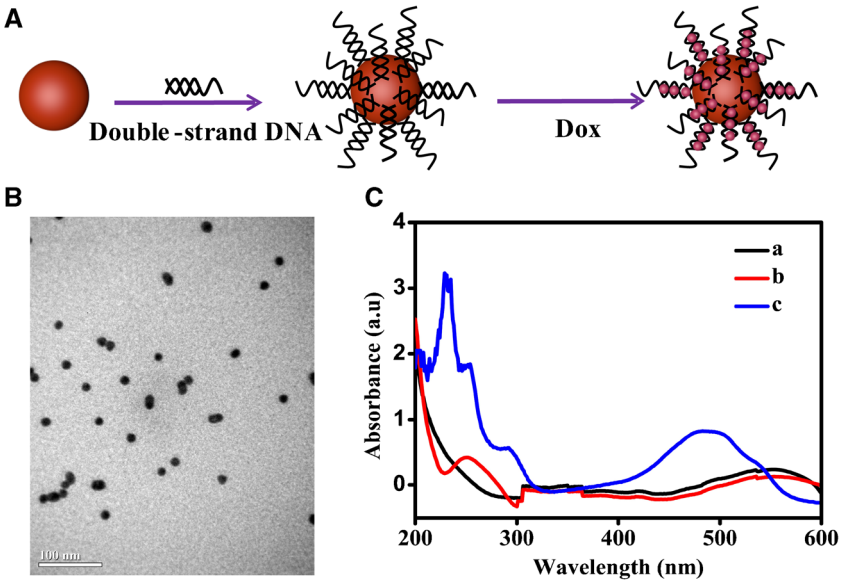

Fig. 1 Characterization of AuNPs and DSNA tags. **a** The self-assembled procedure for DSNAs. **b** TEM image of AuNPs, Scale bars: 100 nm. **c** UV–vis absorption spectrums of (a) AuNPs, (b) SNAs, (c) DSNAs. For particle sizes, standard deviations (± 1.5) and the number of particles (n = 35)

the other probe ET. Thus, automatic motions of the elongated swing arm along the pre-designed track can be propelled by DNA strand displacement. As a result, numbers of FT probes attach to the modified electrode surface by forming ET-FT complex for capturing the electrochemical indicator DSNA, leading to the production of significantly amplified output signal. The FNA nanomachine and DSNA tags offer a novel signal amplification pattern for evaluating telomerase activity.

Choice of materials

These materials, including SNAs, tetrahedron framework, and Au electrode, were used to perform the detection of telomerase activity. Compared to DNA origami, tetrahedron framework not only owns simple assembly (four short DNA strands), but improve the sensitivity and stability of the biosensors [22–24]. SNAs have many advantages, such as low toxicity, larger surface areas, and good dispersibility and stability [29, 30]. Compared with other nanomaterial electrodes, Au electrode displays high conductivity and high affinity with sulfydryl groups, which load easily with thiolated DNA. Hence, these materials are chose to construct the electrochemical biosensor for the detection of telomerase activity.

Characterization of AuNPs and DSNA tags

The schematic diagram of the self-assembled process of DSNA is illustrated in Fig. 1a. The synthetic AuNPs and the

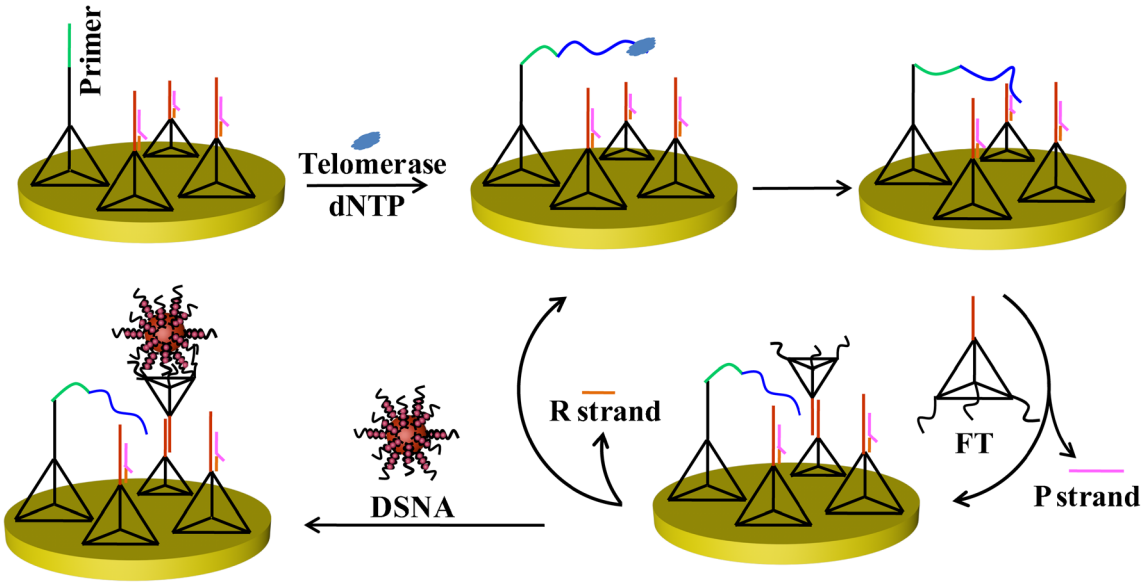

Scheme 1 Schematic illustration of target induced FNA nanomachine with DSNA tags for electrochemical detection of telomerase activity.

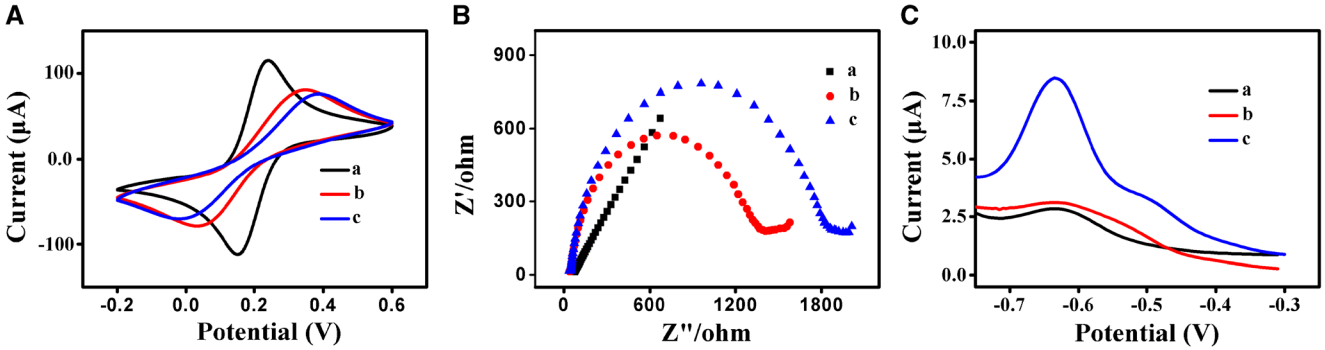

Fig. 2 **a** CV and **b** EIS representations of the modified gold electrode at different conditions: (a) bare gold electrode, (b) ET/PT/bare gold electeode, (c) telomerase + FT + ET/PT/bare gold electeode. **c** Testing the feasibility of the method. SWV results at different reaction conditions: (a) DSNAs + ET/PT/gold electrode, (b) FT + DSNAs + ET/PT/gold electrode, and (c) telomerase + FT + DSNAs + ET/PT/gold electrode. The concentrations of DSNAs and FT are 100 nM and 250 nM, respectively. Telomerase contract is from 1000 HeLa cells mL^{-1}

assembly process of DSNA were verified by the transmission electron microscopic (TEM) image and UV-vis absorption spectrums, respectively. As shown in Fig. 1b, the synthesized AuNPs show good uniformity and dispersity, and the average diameter of the AuNPs is 15 nm. As seen in Fig. 1c, the peak of DNA at 260 nm in the UV-vis spectrum of SNAs shows that DNA binds to AuNPs (curve b) compared to the peak of AuNPs (curve a). Curve c shows the UV-vis spectrum of DSNAs.

Characterization of the modified electrode

The modification of the electrode at each step was studied by CV and EIS, respectively. As shown in Fig. 2a, bare gold electrode exhibits a pair of well-defined current peaks (curve a) on account of the good electron transfer capability. After modification with ET and PT, the peaks distinctly decrease due to the fact that negatively charged DNA is capable of repelling $[Fe(CN)_6]^{3-/4-}$(curve b). In the presence of telomerase and FT, FNA nanomachine is triggered, resulting in the binding of many FTs to the gold electrode. Thus, the CV peaks further reduce (curve C). Then, EIS results are recorded in Fig. 2b. In general, the semicircle size represents the electron transfer limited process in an impedance spectrum. Compared to the bare gold electrode (curve a), the value of electron-transfer resistance (Ret) of ET/PT/bare gold electrode (curve b) significantly enhance. After the operation of telomerase-induced nanomachine, an increased semicircle diameter is observed (curve c), owing to the constructed nanomachine walking that brings more negatively charged FT to the gold electrode surface. The EIS results are consistent with those of CV, suggesting the successful modification of the gold electrode.

Feasibility of the method

To clearly demonstrate the feasibility of the sensing method for telomerase assay, the SWV measurements were carried out under different reaction conditions. Native polyacrylamide gel

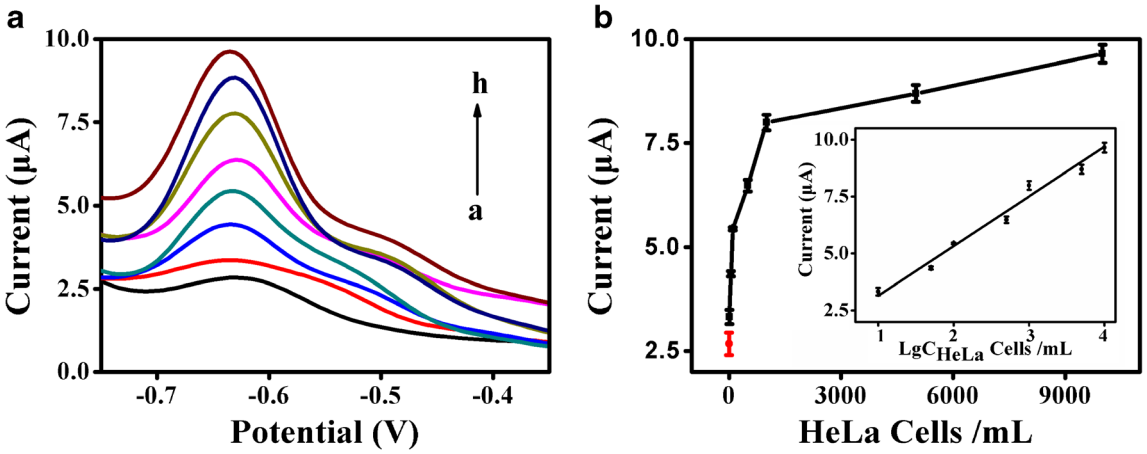

Fig. 3 Evaluation of the sensitivity of the strategy. SWV signals in response to a range of HeLa cell extracts (from a to h): **a** 0, 10, 50, 100, 500, 1.0×10,^{3} 5.0×10,^{3} 1.0×10^4 cells mL^{-1}. **b** Calibration plots of the SWV peak current versus different number of HeLa cells. Insets: linear plots of calibration versus the logarithm of HeLa cell number ranging from 10 cells to1.0×10^4 cells. SWV were carried out from −0.80 to −0.3 V with amplitude of 25 mV and frequency of 25 Hz, typically measured at around −0.63 mV (Ag/AgCl). All data expressed as mean ± standard variation ($n = 3$)

Table 1 Comparison of our method with other methods for the detection of telomerase activity

Method applied	Materials used	LOD	Reference
Electrochemistry	Hairpin probe	40 cells mL^{-1}	[11]
Fluorescence	Endonuclease-driven walking	90 cells μL^{-1}	[20]
Electrochemistry	Gold nanorods	52.8 cells mL^{-1}	[36]
Fluorescence	Exponential rolling circle amplification	1 cells mL^{-1}	[37]
ECL	Ruthenium Complex doped MOF	11 cells mL^{-1}	[38]
Fluorescence	graphene quantum dot and GO	10 cells mL^{-1}	[39]
Electrochemistry	FNA nanomachine with DSNA tags	2 cells mL^{-1}	This work

ECL Electrochemiluminescence, *MOF* Metal-Organic Frameworks, *FNA* Framework nucleic acids, *DSNA* doxorubicin-spherical nucleic acids, *GO* graphene oxide

electrophoresis (PAGE) was carried out for characterizing the formation of DNA tetrahedron (Fig. S1). As shown in Fig. 2c, in the absence of the telomerase extracts and FT, ignorable current peak has been observed because ET and PT modified gold electrodes cannot absorb DSNA tags (curve a). Then the SWV result of the modified electrode without telomerase extracts is also recorded (curve b), which barely changes in comparison to curve a due to that the FNA nanomachine cannot be initiated, leading to the result that no DSNA tags bind to the modified electrode. However, once telomerase extracts is introduced, the extended swing arm binds to ET and triggers nanomachine walking, subsequently forming ET-FT complex, and then capturing the DSNA tags, resulting a well-defined current peak of Dox appeared at about −0.632 V (curve c), powerfully demonstrating that the DSNA tags captured on the electrode surfaces is attribute to the operation of target-induced nanomachine. Therefore, the results show that the strategy is feasible and offers a novel method for telomerase detection.

Optimization of the assay conditions

To get a higher sensitivity, the following parameters were optimized: (a) ratio of PT to ET; (b) incubation temperature; (c) reaction time; (d) concentration of dsDNA bound to AuNP; (e) density of ET/PT on the electrode. Respective data and Figures are given in the ESM. The following experimental conditions were found to give best results: (a) Best ratio of PT to ET: 1/9; (b) Optimal incubation temperature: 37 °C; (c) Optimal incubation time: 45 min; (d) Best concentration of dsDNA bound to AuNP: 100 nM; (e) the densities of ET and PT on the electrode were 1 μM and 100 nM, respectively.

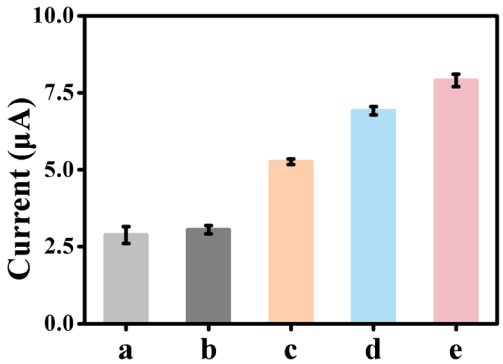

Fig. 4 Telomerase activity detection of different cell lines. SWV signals in response to telomerase activity of different cell line extracts (equivalent to 1000 cells): (a) HL-7702 cells, (b) heated telomerase extracts, (c) MCF-7 cells, (d) HepG2 cells, (e) HeLa cells. All data expressed as mean ± standard variation ($n = 3$)

Sensitivity

Under the optimized reaction conditions, the sensitivity of the sensing strategy for various concentrations of telomerase extracted from HeLa cells was evaluated. As shown in Fig. 3a, with the increase of telomerase extracts corresponding to from 0 cell to 10^4 HeLa cells, more FT-ET complexes are formed to capture DSNA tags, which are directly reflected by the stepwise increased current intensity. The relationships between increased peak currents and cell numbers are used for plotting calibration plot (Fig. 3b). A good linear relationship is constructed for the cell numbers ranging from 10 to 10^4 HeLa cells with the regression equation as follows:

$$y = 2.18\ \lg C + 0.96\ \left(R^2 = 0.96\right)$$

in which y stands for the electrochemical peak, and C is the HeLa cell number mL^{-1}. The detection limit of 2 cells mL^{-1} is calculated based on the average signal of blank plus three times of the standard deviation. The electrochemical sensitivity is 0.104 $\mu A \cdot \mu M^{-1} \cdot cm^{-2}$. This method shows superior sensitivity to those of previously reported telomerase detection methods (Table 1).

Telomerase detection in different cell lines

It is known that different cancer cells show obviously difference in the expression levels of telomerase. To evaluate the capacity to detect telomerase activities in various cell lines, the method was applied to test HepG2, HeLa, MCF-7 and normal cells (HL-7702), respectively. As described in Fig. 4, compared with HL-7702, the current signals given by HepG2,

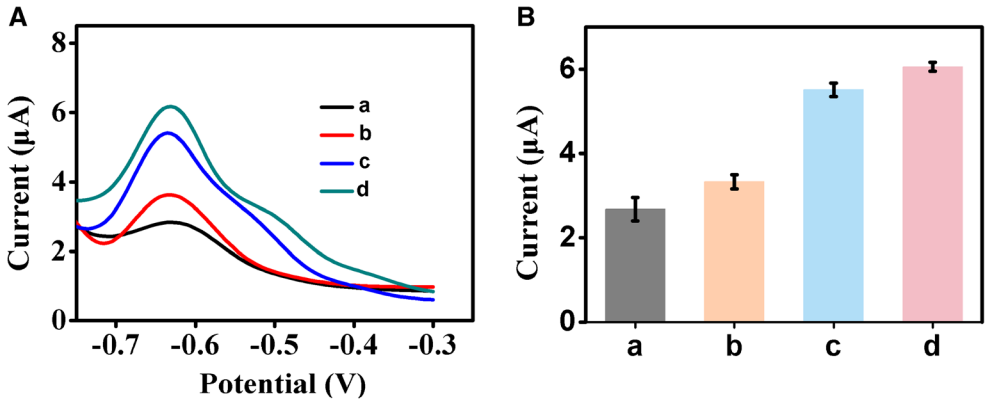

Fig. 5 Detection of telomerase activity in the mixed cells. **a** SWV signals and **b** the current intensities in response to different diluted times: (a) the blank control, (b) 100-folds, (c) 10-folds, (d) 5-folds. The mixture comprising of HL-7702 and HeLa cells has 1000 cells mL^{-1} in total. SWV were carried out from −0.80 to −0.3 V with amplitude of 25 mV and frequency of 25 Hz. All data expressed as mean ± standard variation ($n = 3$)

HeLa, and MCF-7 are raised. However, when the telomerase extracts from these cancer cells are heated at 95 °C 10 min, the telomerase level is almost the same with normal cells. In addition, the telomerase expression levels follow the descending order of HeLa > HepG2 > MCF-7, which is in accord with previous reported studies [40]. These results demonstrate that the strategy can distinguish cancer cell lines via their different telomerase activity levels.

Cancer cell detection in cell mixture

Generally, cancer cells are blended with many normal cells in clinical samples. To assess the clinical applicability of the sensing method, we investigated its capacity for discerning cancer cells in cell mixture. Firstly, HeLa cells are diluted 5-folds, 10-folds, and 100-folds with normal cells (HL-7702), respectively. Then the cell extracts of these compounds are used to analyze telomerase activity. As seen in Fig. 5, the current intensity enhance with the decrease of HeLa cells diluted times. In comparison to the blank control that only includes HL-7702 cells, the electrochemical signal produced by 100-folds diluted HeLa cells is distinctly increased. These results prove that this sensing method can detect infrequent cancer cells from abundant normal cells. Hence, the method has potential clinical applications.

Conclusion

We describe a method based on framework nucleic acid (FNA) nanomachine with doxorubicin-spherical nucleic acid (DSNA) tags for the determination of telomerase activity. Under the optimized conditions, the method revealed a wide dynamic range and a low detection limit for the detection of telomerase activity from HeLa cells. The telomerase activities of different kinds of cancer cells were sensitively and easily measured. The sensing system was also used for telomerase activity of cancer cells detection in accumulated normal cells with satisfactory results. However, there are challenges for this method applied to clinical samples, such as high working potential and the interferences of complex compositions in body fluid.

Acknowledgments This work was supported by Health Commission of Henan Province (No.2018020495).

Compliance with ethical standards

The author(s) declare that they have no competing interests.

References

1. Cohen SB, Graham ME, Lovrecz GO, Bache N, Robinson PJ, Reddel RR (2007) Protein composition of catalytically active human telomerase from immortal cells. Science 315:1850–1853
2. Shay JW, Wright WE (2019) Telomeres and telomerase: three decades of progress. Nat Rev Genet 20:299–309
3. Wang LJ, Ma F, Tang B, Zhang CY (2017) Sensing telomerase: from detection to imaging. Chem Sci 8:2495–2502
4. Zhou XM, Xing D (2012) Assays for human telomerase activity: progress and prospects. Chem Soc Rev 41:4643–4656
5. Lee ST, Rahman R, Muthoosamy K, Mohamed NAH, Su X, Tayyab S, New SY (2019) Amplification-free and direct fluorometric determination of telomerase activity in cell lysates using chimeric DNA-templated silver nanoclusters. Microchim Acta 186:81
6. Ma F, Wang TT, Jiang L, Zhang CY (2019) Ultrasensitive detection of telomerase activity in lung cancer cells with quencher-free molecular beacon-assisted quadratic signal amplification. Anal Chim Acta 1053:112–130
7. Peng M, Na N, Ouyang J (2019) A fluorescence light-up silver nanocluster beacon modulated by metal ions and its application in telomerase-activity detection. Chemistry 25(14):3598–3605
8. Yang H, Liu A, Wei M, Liu Y, Lv B, Wei W, Zhang Y, Liu S (2017) Visual, label-free telomerase activity monitor via enzymatic etching of gold nanorods. Anal Chem 89:12094–12100

9. Wang D, Guo R, Wei Y, Zhang Y, Zhao X, Xu Z (2018) Sensitive multicolor visual detection of telomerase activity based on catalytic hairpin assembly and etching of Au nanorods. Biosens Bioelectron 122:247–253
10. Meng F, Xu Y, Dong W et al (2018) A PCR-free voltammetric telomerase activity assay using a substrate primer on a gold electrode and DNA-triggered capture of gold nanoparticles. Microchim Acta 185:398
11. Wang G, Wang H, Cao S, Xiang W, Li T, Yang M (2019) Electrochemical determination of the activity and inhibition of telomerase based on the interaction of DNA with molybdate. Microchim Acta 186:96
12. Zhang X, Lou X, Xia F (2017) Advances in the detection of telomerase activity using isothermal amplification. Theranostics 7: 1847–1862
13. Kim J, Jang D, Park H, Jung S, Kim DH, Kim WJ (2018) Functional-DNA-driven dynamic nanoconstructs for biomolecule capture and drug delivery. Adv Mater 30:1707351
14. Scalise D, Schulman R (2019) Controlling matter at the molecular scale with DNA circuits. Annu Rev Biomed Eng 21:469–493
15. Wang H, Wang H, Liu C, Duan X, Li Z (2016) Ultrasensitive detection of telomerase activity in a single cell using stem-loop primer-mediated exponential amplification (SPEA) with near zero nonspecific signal. Chem Sci 7:4945–4950
16. Li CC, Zhang Y, Liu WJ, Zhang CY (2018) A triple-amplification strategy for sensitive detection of telomerase at the single-cell level. Chem Commun 54:9317–9320
17. Wang W, Huang S, Li J, Rui K, Bi S, Zhang JR, Zhu JJ (2017) Evaluation of intracellular telomerase activity through cascade DNA logic gates. Chem Sci 8:174–180
18. Xu X, Wang L, Li K, Huang Q, Jiang W (2018) A smart DNA tweezer for detection of human telomerase activity. Anal Chem 90: 3521–3530
19. Wang Z, Hou R, Loh IY (2019) Track-walking molecular motors: a new generation beyond bridge-burning designs. Nanoscale 11: 9240–9263
20. Huang J, Zhu L, Ju H, Lei J (2019) Telomerase triggered DNA Walker with a superhairpin structure for human telomerase activity sensing. Anal Chem 91:6981–6985
21. Li X, Cheng W, Li D, Wu J, Ding X, Cheng Q, Ding S (2016) A novel surface plasmon resonance biosensor for enzyme-free and highly sensitive detection of microRNA based on multi component nucleic acid enzyme (MNAzyme)-mediated catalyzed hairpin assembly. Biosens Bioelectron 80:98–104
22. Yang F, Li Q, Wang L, Zhang GJ, Fan C (2018) Framework-nucleic-acid-enabled biosensor development. ACS Sens 3:903–919
23. Ge Z, Gu H, Li Q, Fan C (2018) Concept and development of framework nucleic acids. J Am Chem Soc 140:17808–17819
24. Ye D, Zuo X, Fan C (2018) DNA nanotechnology-enabled interfacial engineering for biosensor development. Annu Rev Anal Chem 11:171–195
25. Bui H, Shah S, Mokhtar R, Song T, Garg S, Reif J (2018) Localized DNA hybridization chain reactions on DNA origami. ACS Nano 12:1146–1155
26. He L, Lu D, Liang H, Xie S, Zhang X, Liu Q, Yuan Q, Tan W (2018) mRNA-initiated, three-dimensional DNA amplifier able to function inside living cells. J Am Chem Soc 140:258–263
27. Yan T, Zhu L, Ju H, Lei J (2018) DNA-Walker-induced allosteric switch for tandem signal amplification with palladium nanoparticles/metal-organic framework tags in electrochemical biosensing. Anal Chem 90:14493–14499
28. Chinen AB, Guan CM, Ko CH, Mirkin CA (2017) The impact of protein corona formation on the macrophage cellular uptake and biodistribution of spherical nucleic acids. Small 13(16):1603847
29. Zhang K, Hao L, Hurst SJ, Mirkin CA (2012) Antibody-linked spherical nucleic acids for cellular targeting. J Am Chem Soc 134(40):16488–16491
30. Tan X, Lu X, Jia F, Liu X, Sun Y, Logan JK, Zhang K (2016) Blurring the role of oligonucleotides: spherical nucleic acids as a drug delivery vehicle. J Am Chem Soc 138:10834–10837
31. Bagalkot V, Farokhzad OC, Langer R, Jon S (2006) An aptamer-doxorubicin physical conjugate as a novel targeted drug-delivery platform. Angew Chem Int Ed Engl 45(48):8149–8152
32. Liu J, Lu Y (2006) Preparation of aptamer-linked gold nanoparticle purple aggregates for colorimetric sensing of analytes. Nat Protoc 1: 246–252
33. Jiang Q, Song C, Nangreave J, Liu X, Lin L, Qiu D, Wang ZG, Zou G, Liang X, Yan H, Ding B (2012) DNA origami as a carrier for circumvention of drug resistance. J Am Chem Soc 134(32):13396–13403
34. Qian R, Ding L, Yan L, Lin M, Ju H (2014) Smart vesicle kit for in situ monitoring of intracellular telomerase activity using a telomerase-responsive probe. Anal Chem 86(17):8642–8648
35. Haiss W, Thanh NT, Aveyard J, Fernig DG (2007) Determination of size and concentration of gold nanoparticles from UV-vis spectra. Anal Chem 79(11):4215–4221
36. Wang L, Meng T, Yu G, Wu S, Sun J, Jia H, Wang H, Yang X, Zhang Y (2019) A label-free electrochemical biosensor for ultrasensitively detecting telomerase activity based on the enhanced catalytic currents of acetaminophen catalyzed by au nanorods. Biosens Bioelectron 124-125:53–58
37. Li X, Cui Y, Du Y, Tang A, Kong D (2019) Label-free telomerase detection in single cell using a five-base telomerase product-triggered exponential rolling circle amplification strategy. ACS Sens 4(4):1090–1096
38. Xiong C, Liang W, Zheng Y, Zhuo Y, Chai Y, Yuan R (2017) Ultrasensitive assay for telomerase activity via Selfenhanced Electrochemiluminescence ruthenium complex doped metal-organic frameworks with high emission efficiency. Anal Chem 89:3222–3227
39. Kazemi E, Bagheri H, Norouzian D (2019) A turn-on graphene quantum dot and graphene oxide based fluorometric aptasensor for the determination of telomerase activity. Microchim Acta 186(12):785
40. He C, Liu Z, Wu Q, Zhao J, Liu R, Liu B, Zhao T (2018) Ratiometric fluorescent biosensor for visual discrimination of cancer cells with different telomerase expression levels. ACS Sens 3: 757–762